ORIENTAL JOURNAL OF CHEMISTRY
An International Open Access, Peer Reviewed Research Journal
www.orientjchem.org
ISSN: 0970-020 X
CODEN: OJCHEG
2024, Vol. 40, No.(5):
Pg. 1329-1339

Characterization, Synthesis, and Antimicrobial activities of Quinazoline Derivatives [EMNEDAQZHO] and their Metal Ion Complexes

SHEEBA. M. SHAIKH[1*] and MAJOR RAHUL. R. WAGH[2]

[1,2]Patkar Varde College, Affiliated to Mumbai University, India
*Corresponding author E-mail: sheebushaikh055@gmail.com,
drrahulwagh.123@gmail.com

http://dx.doi.org/10.13005/ojc/400515

(Received: September 14, 2024; Accepted: October 20, 2024)

ABSTRACT

The synthesis, characterization, and antimicrobial evaluation of quinazoline derivatives and their metal ion complexes have garnered significant attention in medicinal chemistry due to their potential therapeutic applications. This study reports the preparation of novel quinazoline derivatives through a deaminative coupling reaction between substituted acetonaphthone and 2-methyl-4H-1,3-benzoxazine-4-one using different amines. Additionally, the coordination behavior of these quinazoline derivatives with metal ions such as Co^2, Ni^2, Cu^2, and Zn^2 was explored, resulting in stable metal-ligand complexes. The structural and physico-chemical properties of the synthesized ligand [EMNEDAQZHO] and its metal complexes were analyzed using a combination of volumetric techniques and advanced characterization methods, including FTIR, ^{1}H NMR, UV-Vis, TGA, and mass spectrometry. Thermogravimetric analysis (TGA) was employed to assess thermal stability, metal content, and moisture loss in the complexes. The antimicrobial activities of the quinazoline Schiff base ligand [EMNEDAQZHO] and its metal complexes were evaluated against a range of bacterial and fungal strains, with minimum inhibitory concentrations (MIC) determined at varying concentrations. This study successfully demonstrates the synthesis of quinazoline derivatives [AMQZHO] and Schiff base [EMNEDAQZHO], as well as their metal ion complexes, through both established and novel synthetic methodologies. The antimicrobial assays revealed that coordination with metal ions significantly enhances the biological activity of the ligands, making these complexes promising candidates for the development of new antimicrobial agents in pharmaceutical applications.

Keywords: Quinazoline derivatives, Schiff base, Metal ion complexes, Antimicrobial activity, Synthesis, Characterization, Deaminative coupling, Thermal stability.

INTRODUCTION

Nitrogen- and sulfur-containing heterocyclic compounds have garnered significant interest due to their extensive therapeutic and pharmacological potential. Among these, quinazoline stands out as a highly promising structure, largely owing to its broad spectrum of biological activities and relatively low side effects[1]. Quinazoline (C=H=N) is a heterocyclic compound composed of a fused benzene and pyrimidine ring, commonly referred to as

1,3-diazanaphthalene. It typically appears as a light yellow crystalline solid[2].

The first synthesis of quinazoline was achieved in 1895 by Bischler and Lang through the decarboxylation of a 2-carboxy derivative. A more notable synthetic route, the Niementowski reaction, involves the reaction of anthranilic acid with amides to form 4-oxo-3,4-dihydroquinazolines[3]. Quinazoline isomers, such as quinoxaline, cinnoline, and phthalazine, further extend the diversity of this compound's chemical behavior[4]. Quinazoline structures have been associated with various pharmacological activities, including anti-obesity, antiviral, and nematicidal effects, as well as serving as A2A adenosine receptor antagonists[5]. Notably, quinazoline derivatives have been discovered in over 200 naturally occurring alkaloids, sourced from plants, microorganisms, and animals[6]. One well-known quinazoline alkaloid, vasicine (also called peganine), was isolated from Adhatoda vasica in 1888 and is celebrated for its bronchodilator properties[7]. These derivatives exhibit a broad range of biological activities, including antibacterial, antifungal, anti-inflammatory, antidiabetic, antipsychotic, antimalarial, and antituberculosis actions. Additionally, they serve as inhibitors of enzymes like poly-(ADP-ribose) polymerase (PARP), thymidylate synthase, and tyrosine kinase, thus showing significant potential in cancer treatment, particularly hepatocellular carcinoma[8]. Several quinazoline-based compounds have been approved for therapeutic use, such as Terazosin hydrochloride, Prazosin hydrochloride, and Doxazosin mesylate. Furthermore, quinazoline derivatives like Erlotinib, Gefitinib, Lapatinib, Vandetanib, and Afatinib have gained USFDA approval for the treatment of various cancers[9]. These approvals underscore the ongoing research and clinical focus on quinazoline derivatives in organic synthesis and medicinal chemistry[10].

The discovery of quinazoline compounds dates back to 1869 when Griess synthesized 2-cyano-3,4-dihydro-4-oxoquinazoline by reacting cyanogen with 2-aminobenzoic acid, which he initially identified as bicyanoamido benzoyl[11]. Bischler and Lang synthesized the parent quinazoline molecule in 1895 by decarboxylating a 2-carboxy quinazoline derivative[4]. Gabriel further improved the synthesis methods in 1903[12], and the name "quinazoline" was subsequently adopted to represent this fused benzene-pyrimidine ring structure[2].

In recent years, advancements in the synthesis and modification of quinazoline derivatives have led to research on their coordination with metal ions, particularly transition metals such as Co^{+2}, Cu^{+2}, Ni^{+2}, and Zn^{+2}. These metal complexes significantly enhance the pharmacological activities of quinazoline derivatives, paving the way for new drug development opportunities[13].

This review aims to highlight the most recent developments in the synthesis, characterization, and pharmacological applications of quinazoline derivatives and their metal complexes. By providing a comprehensive analysis, this review hopes to stimulate further research and innovation in quinazoline-based drug discovery within medicinal chemistry[14].

MATERIAL AND METHODOLOGY

2-amino-benzoic acid, Acetic anhydride, 2-methyl-4H-1,3-benzoxazine-4-one (MHBZ) (from Step 1), Hydrazine hydrate (99%), 3-amino-2-methylquinazolin-4-(3H)-one (AMQZHO) (from Step 2), Substituted acetonaphthones, Ethyl alcohol, Acetic acid , Water bath or heating mantle, Round-bottom flask, Reflux condenser, Recrystallization apparatus, Weighing balance, Solvent (e.g., ethanol, methanol, propanol), Filter paper, Ice-bath.

Methodology

Synthesis of Quinazoline Derivative (EMNEDAQZHO) and Its Transition Metal Complexes

The synthesis of the quinazoline derivative (EMNEDAQZHO) and its transition metal complexes with Zn, Cu, Ni, and Co was achieved using substituted carboxylic acids as starting materials in the presence of a suitable catalyst. The preparation involved several steps, as outlined below:

Step 1: Synthesis of 2-Methyl-4H-1,3-benzoxazine -4-one (MHBZ) (2a)

In a 250 mL round-bottom flask, 2-amino-benzoic acid (0.01 M, 2 g) was combined with 10 mL of acetic anhydride to create an acidic environment. The mixture was refluxed for 3 h using a water bath or heating mantle. After completion, the mixture was allowed to cool, and the resulting solid was filtered and weighed[15].

Step 2: Synthesis of 3-Amino-2-methylquinazolin-4-(3H)-one (AMQZHO) (2b)

A solution of the compound synthesized in Step 1 (0.02 M, 3 g) in 15 mL of absolute ethanol was prepared. To this, hydrazine hydrate (99%) (10 mL) was added. The reaction mixture was refluxed for 27 h, followed by cooling. The solid product formed was filtered and recrystallized from water to obtain pure 3-amino-2-methylquinazolin-4-one[16].

Step 3: Preparation of Quinazoline-based Schiff Base (EMNEDAQZHO) (2ab)

In a 50 mL round-bottom flask, a solution of 3-amino-2-methyl-3H-quinazolin-4-one (0.01 M) and substituted acetonaphthones (0.01 M) was prepared by dissolving them in 15 mL of ethanol. Acetic acid (0.001 M) was then added as a catalyst, and the mixture was refluxed for 2–3 hours. After the reaction cooled down, the Schiff base derivative (EMNEDAQZHO) was collected[17].

Metal Complex Preparation Method

Preparation of Zn(II), Cu(II), Ni(II), and Co(II) Metal Complexes of EMNEDAQZHO

Synthesis of Zn(II) Metal Complex (L-Zn)

To synthesize the Zn^{+2} metal complex of EMNEDAQZHO (L-Zn), dissolve 1.2 equivalents of the EMNEDAQZHO Schiff base in hot ethanol. Add 1.1 equivalents of $ZnCl_2 \bullet 5H_2O$ to the solution with continuous stirring. Reflux the mixture for 2-3 h to ensure complete coordination. Upon cooling to room temperature, the Zn^{+2} complex L-Zn will precipitate out. Collect the precipitate by filtration, wash it with aqueous ethanol to remove impurities, and dry it under vacuum to obtain the final product[18].

Synthesis of Cu(II) Metal Complex (L-Cu)

To synthesize the Cu^{+2} metal complex of EMNEDAQZHO (L-Cu), dissolve 1.2 equivalents of the EMNEDAQZHO Schiff base in hot ethanol. Add 1.1 equivalents of $CuSO_4 \bullet 5H_2O$ to the solution with continuous stirring. Reflux the mixture for 2-3 h to ensure complete coordination. Upon cooling to room temperature, the Cu^{+2} complex L-Cu will precipitate out. Collect the precipitate by filtration, wash it with aqueous ethanol to remove impurities, and dry it under vacuum to obtain the final product[19].

Synthesis of Ni(II) Metal Complex (L-Ni)

To synthesize the Ni^{+2} metal complex of EMNEDAQZHO (L-Ni), dissolve 1.2 equivalents of the EMNEDAQZHO Schiff base in hot ethanol. Add 1.1 equivalents of $NiCl_2 \bullet 6H_2O$ to the solution with continuous stirring. Reflux the mixture for 2-3 h to ensure complete coordination. Upon cooling to room temperature, the Ni^{+2} complex L-Ni will precipitate out. Collect the precipitate by filtration, wash it with aqueous ethanol to remove impurities, and dry it under vacuum to obtain the final product[20].

Synthesis of Co(II) Metal Complex (L-Co)

To synthesize the Co^{+2} metal complex of EMNEDAQZHO (L-Co), dissolve 1.2 equivalents of the EMNEDAQZHO Schiff base in hot ethanol. Add 1.1 equivalents of $Co(NO_3)_2 \bullet 6H_2O$ to the solution with continuous stirring. Reflux the mixture for 2-3 h to ensure complete coordination. Upon cooling to room temperature, the Co^{+2} complex L-Co will precipitate out. Collect the precipitate by filtration, wash it with aqueous ethanol to remove impurities, and dry it under vacuum to obtain the final product[21].

RESULTS AND DISCUSSION

Ligand:(E)-2-methyl-3-(1-(naphthalen-1-yl)ethylideneamino)quinazolin-4(3H)-one (EMNEDAQZHO), Green colour product, m.p.-230°C, λ_{max} at 430nm.

Zn-Metal (L-Zn): Zn comlex of (E)-2-methyl-3-(1-(naphthalen-1-yl)ethylideneamino) quinazolin-4(3H)-one (EMNEDAQZHO), buff color complex m.p. at>280°C, λ_{max} at 450nm.

Cu-Metal (L-Cu): Cu comlex of (E)-2-methyl-3-(1-(naphthalen-1-yl)ethylideneamino) quinazolin-4(3H)-one (EMNEDAQZHO), greenish blue color complex m.p. at>280°C, λ_{max} at 450nm.

Ni-Metal (L-Ni): Ni comlex of (E)-2-methyl-3-(1-(naphthalen-1-yl)ethylideneamino) quinazolin-4(3H)-one (EMNEDAQZHO), Buff green color complex, m.p. at >280°C, λ_{max} at 450nm.

Co-Metal (L-Co): Co comlex of (E)-2-methyl-3-(1-(naphthalen-1-yl)ethylideneamino) quinazolin-4(3H)-one (EMNEDAQZHO), light orange color complex, m.p. at >280°C, λ_{max} at 450nm.

FTIR Data

The FTIR spectrum of the ligand displayed distinct peaks corresponding to C-N stretching,

aromatic C-H stretching, aromatic C=C stretching, and C-O stretching vibrations. Upon forming complexes with metal ions, shifts in these peak positions, as well as the emergence or loss of specific peaks, were noted, suggesting the coordination of metal ions with the functional groups of the ligand[22-23].

The FTIR spectrum of the ligand (Fig. 1.1) shows characteristic peaks at 3232.98 cm^{-1} and 3192.45 cm^{-1}, indicating C-N stretching, along with 3043.06 cm^{-1} for aromatic C-H stretching, 1664.29 cm^{-1} for aromatic C=C stretching, 1547.80 cm^{-1} for C-O stretching, 1269.50 cm^{-1} for C-N stretching, 1092.04 cm^{-1} for C-O stretching, and 780.47 cm^{-1}, likely representing out-of-plane C-H stretching, potentially from an aliphatic CH– group.

Upon complexation with Zn (Fig. 1.2), the peaks shift to 3191.60 cm^{-1} and 3042.73 cm^{-1} for C-N stretching, with a peak at 1664.34 cm^{-1} for aromatic C=C stretching and 1547.53 cm^{-1} representing C-O stretching and possibly O-M bond formation. Additional peaks at 1440.10 cm^{-1} for C-H bending, 1091.24 cm^{-1} for C-O stretching, and 780.39 and 569.06 cm^{-1} for out-of-plane C-H stretching were observed.

For the Cu complex (Fig. 1.3), the spectrum shows a new broad peak at 3446.51 cm^{-1} for O-H stretching, along with 3337.83 cm^{-1} for C-N stretching, 1599.13 cm^{-1} for C-O stretching/O-M bond, 1150.05 cm^{-1} for aromatic C=C stretching, and additional peaks at 991.19 and 602.81 cm^{-1} for out-of-plane C-H stretching, likely due to an aliphatic CH_3 group.

The Ni complex (Fig. 1.4) presents C-N stretching peaks at 3236.11 cm^{-1}, 3190.90 cm^{-1} (C-N/C-H stretching), and 3043.47 cm^{-1} for C-N stretching. Peaks at 1664.50 cm^{-1} for C-O stretching/aromatic C=C stretching and 1546.67 cm^{-1} for C-O stretching/O-M bond were observed, with an additional peak at 1092.02 cm^{-1} for aromatic C=C stretching and 779.92 cm^{-1} for out-of-plane C-H stretching.

In the Co complex (Fig. 1.5), a broad peak at 3445.31 cm^{-1} indicates O-H stretching, with peaks at 3192.56 cm^{-1} for C-N/C-H stretching and 3043.52 cm^{-1} for aromatic C-H stretching. Further peaks appear at 1664.65 cm^{-1} for C-O stretching/aromatic C=C stretching, 1547.35 cm^{-1} for C-O stretching/O-M bond, and 1269.39 and 1092.23 cm^{-1} for aromatic C=C stretching. Out-of-plane C-H stretching peaks were noted at 779.33,595.58, and 569.54 cm^{-1}.

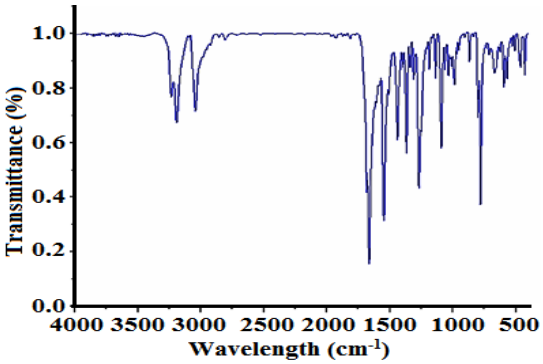

Fig. 1.1

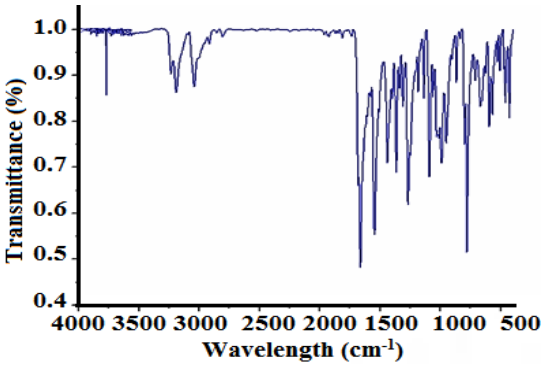

Fig. 1.2

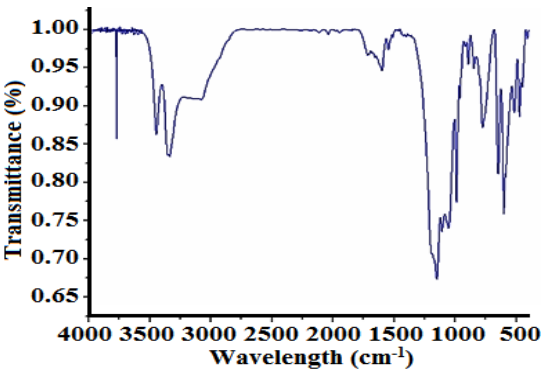

Fig. 1.3

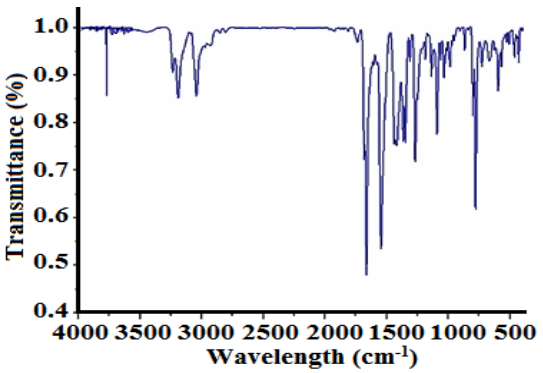

Fig. 1.4

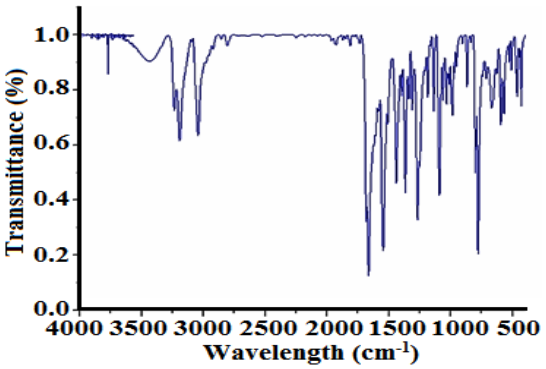

Fig.1.5

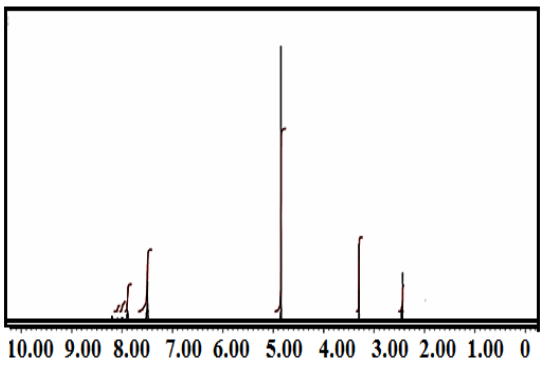

Fig. 2.1

NMR Spectra

The ^{1}HNMR spectrum of the ligand exhibited distinct peaks at various chemical shifts, indicative of different proton environments within the molecule. Singlets, doublets, and multiplets were observed, corresponding to protons in different chemical environments and neighbouring proton interactions. By comparing the experimental data with known chemical shifts and coupling constants, the molecular structure of the ligand was elucidated[24-25].

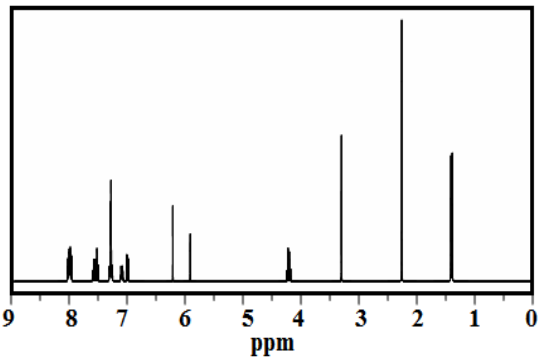

Fig. 2.2

Ligand : Fig. 2.1- 2.52ppm (singlet), 3.35ppm (singlet), 7.5ppm (doublet), 7.59ppm (doublet), 7.65ppm (multiplet), 7.9ppm (multiplet), 8.0ppm (multiplet), 8.1ppm(multiplet) , 8.2ppm(multiplet).

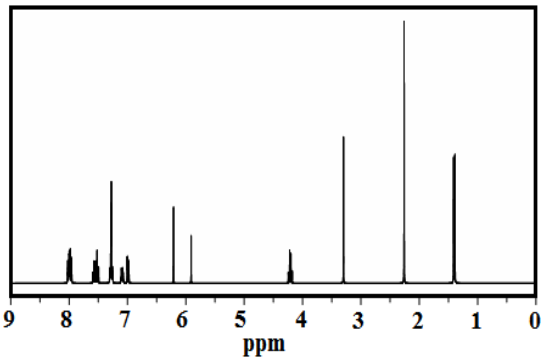

Fig. 2.3

L-Zn Complex: Fig. 2.2-1.42ppm (doublet), 2.25ppm (singlet), 3.3ppm (singlet), 4.25ppm (Multiplet), 5.9ppm (singlet), 6.2ppm(singlet), 7.0ppm, 7.2ppm, 7.3ppm (doublet), 7.6ppm (multiplet), 8.0ppm (multiplet).

L-Cu Complex: Fig. 2.3-1.42ppm (doublet), 2.25ppm (singlet), 3.3ppm (singlet), 4.25ppm (Multiplet), 5.9ppm (singlet), 6.2ppm(singlet), 7.0ppm, 7.2ppm, 7.3ppm (doublet), 7.6ppm (multiplet), 8.0ppm (multiplet).

L-Ni Complex: Fig. 2.4-1.42ppm (doublet), 2.25ppm (singlet), 3.3ppm (singlet), 4.25ppm (Multiplet), 5.9ppm (singlet), 6.2ppm (singlet), 7.0ppm, 7.2ppm, 7.3ppm (doublet), 7.6ppm (multiplet), 8.0ppm (multiplet).

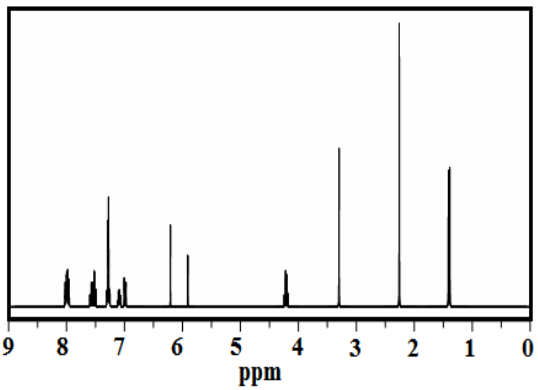

Fig. 2.4

L-Co Complex: Fig. 2.5-1.42ppm (doublet), 2.25ppm (singlet), 3.3ppm (singlet), 4.25ppm (Multiplet), 5.9ppm (singlet), 6.2ppm(singlet), 7.0ppm, 7.2ppm, 7.3ppm (doublet), 7.6ppm (multiplet), 8.0ppm (multiplet).

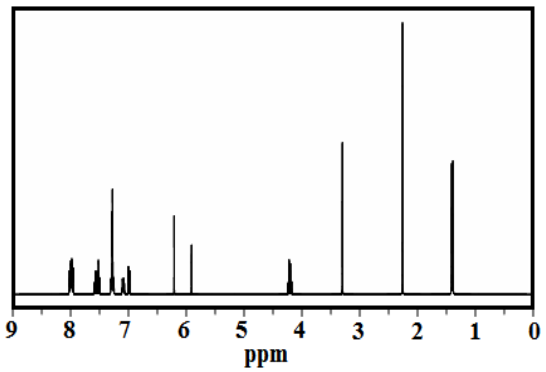

Fig. 2.5

Mass Spectra

L-Ligand: Fig. 3.1-(E)-2-methyl-3-((1-(naphthalen-1-yl)ethylidene)amino)quinazolin-4(3H)-one (molecular formula $C_{21}H_{18}N_3O$), we need to consider the major fragments that could be observed in a mass spectrometry analysis[26-27].

Molecular Ion (M^+): The molecular ion peak corresponds to the intact molecule. This peak is usually the highest mass peak observed in the spectrum.

The molecular weight of $C_{21}H_{18}N_3O$

$C_{21}H_{18}N_3O$: 21×12(C)+18×1(H)+3×14(N)+16(O)=252+18+42+16=328 g/mol. Thus, the molecular ion peak, +would be observed at m/z 328. m/z 328: Molecular ion peak (M^+); m/z 313: Loss of CH_3; m/z 299: Loss of $C{=}CH_3$; m/z 201: Loss of $C_{10}H_7$; m/z 168: Cleavage of the quinazolinone ring; m/z 127: Naphthalene fragment ($C_{10}H_7$); m/z 160: Quinazolinone with a methyl group ($C_9H_8N_2O$).

These peaks represent the most probable fragmentations and their corresponding mass-to-charge ratios (m/z) that you would observe in the mass spectrum of the given compound.

L-Zn Complex: Fig. 3.2-To analyze the mass spectrum of a complex containing two molecules of (E)-2-methyl-3-((1-(naphthalen-1-yl)ethylidene)amino)quinazolin-4(3H)-one and one zinc atom (Zn).

Molecular Weight of One Molecule

$C_{21}H_{18}N_3O$:21×12(C)+18×1(H)+3×14(N)+16(O)=252+18+42+16=328 g/mol. Molecular Weight of Two Molecules: 2×328=656 g/mol. Molecular Weight of Zinc: Zn: 65.38 g/mol (considering the most common isotope) Combined Molecular Weight: 656+65.38=721.38 g/mol. For simplicity in mass spectrometry, we round to the nearest whole number: 722 m/z 722: Combined molecular ion peak (2 molecules + Zn); m/z 707: Loss of CH_3; m/z 693: Loss of $C{=}CH_3$; m/z 595: Loss of $C_{10}H_7$; m/z 562: Cleavage of quinazolinone ring; m/z 394: Loss of one molecule of the compound.

These peaks represent the most probable fragmentations and their corresponding mass-to-charge ratios (m/z) that you would observe in the mass spectrum of the given compound.

L-Cu Complex: Fig. 3.3-To analyze the mass spectrum of a complex containing two molecules of (E)-2-methyl-3-((1-(naphthalen-1-yl) ethylidene)amino)quinazolin-4(3H)-one and one copper atom (Cu).

Molecular Weight of One Molecule

$C_{21}H_{18}N_3O$: 21×12(C)+18×1(H)+3×14(N)+16(O)=252+18+42+16=328 g/mol. Molecular Weight of Two Molecules:2×328=656 g/mol. Molecular Weight of Copper : Cu: 63.55 g/mol (considering the most common isotope) Combined Molecular Weight:656+63.55=719.55 g/mol. For simplicity in mass spectrometry, we round to the nearest whole number: 720. m/z 720: Combined molecular ion peak (2 molecules + Cu); m/z 705: Loss of CH_3; m/z 691: Loss of C=CH; m/z 593: Loss of $C_{10}H_7$; m/z 560: Cleavage of quinazolinone ring; m/z 392: Loss of one molecule of the compound; m/z 328: Single molecule ion peak; m/z 313: Single molecule loss of CH_3; m/z 299: Single molecule loss of $C{=}CH_3$; m/z 201: Single molecule loss of $C_{10}H_7$; m/z 168: Single molecule cleavage of quinazolinone ring; m/z 127: Single molecule naphthalene fragment; m/z 64: Copper ion peak (Cu).

These peaks represent the most probable fragmentations and their corresponding mass-to-charge ratios (m/z) you would observe in the mass spectrum of the given complex.

L-Ni Complex: Fig. 3.4- When two molecules of (E)-2-methyl-3-((1-(naphthalen-1-yl)ethylidene)amino)quinazolin-4(3H)-one form a complex with a metal ion Ni^{+2}.

Molecular Weight of One Ligand Molecule

$C_{21}H_{18}N_3O$: 21×12(C)+18×1(H)+3×14(N)+16(O)=252+18+42+16=328 g/mol. Molecular Weight of Two Ligand Molecules: 2×328=656 g/mol. Molecular Weight of Nickel: Ni: 58.69 g/mol (considering the most common isotope)

Combined Molecular Weight for the Metal Complex: 656+58.69=714.69 g/mol. For simplicity in mass spectrometry, we round to the nearest whole number: 715 m/z 715: Combined molecular ion peak (2 ligands+Ni);m/z 700: Loss of CH_3 from the complex; m/z 686: Loss of $C{=}CH_3$ from the complex; m/z 588: Loss of $C_{10}H_7$ from the complex; m/z 555: Cleavage of quinazolinone ring in the complex; m/z 387: Loss of one ligand molecule; m/z 328: Single ligand molecule ion peak; m/z 313: Single ligand molecule loss of CH_3; m/z 299: Single ligand molecule loss of $C{=}CH_3$; m/z 201: Single ligand molecule loss of $C_{10}H_7$; m/z 168: Single ligand molecule cleavage of quinazolinone ring; m/z 127: Single ligand molecule naphthalene fragment; m/z 59: Nickel or cobalt ion peak (Ni).

These peaks represent the most probable fragmentations and their corresponding mass-to-charge ratios (m/z) that you would observe in the mass spectrum of the metal-ligand complex with Ni^{+2}.

L-Co Complex: Fig. 3.5-When two molecules of (E)-2-methyl-3-((1-(naphthalen-1-yl)ethylidene) amino)quinazolin-4(3H)-one form a complex with a metal ion Co^{+2}.

Molecular Weight of One Ligand Molecule

$C_{21}H_{18}N_3O$: 21×12(C)+18×1(H)+3×14(N)+16(O)=252+18+42+16=328 g/mol. Molecular Weight of Two Ligand Molecules:2×328=656 g/mol. Molecular Weight of Cobalt:Co: 58.93 g/mol (considering the most common isotope) Combined Molecular Weight for the Metal Complex:656+58.93=714.93 g/mol. For simplicity in mass spectrometry, we round to the nearest whole number: 715 m/z 715: Combined molecular ion peak (2 ligands +Co); m/z 700: Loss of CH_3 from the complex; m/z 686: Loss of $C{=}CH_3$ from the complex; m/z 588: Loss of $C_{10}H_7$ from the complex; m/z 555: Cleavage of quinazolinone ring in the complex; m/z 387: Loss of one ligand molecule; m/z 328: Single ligand molecule ion peak; m/z 313: Single ligand molecule loss of CH_3; m/z 299: Single ligand molecule loss of $C{=}CH_3$; m/z 201: Single ligand molecule loss of C10H7; m/z 168: Single ligand molecule cleavage of quinazolinone ring; m/z 127: Single ligand molecule naphthalene fragment; m/z 59: Nickel or cobalt ion peak (Co).

These peaks represent the most probable fragmentations and their corresponding mass-to-charge ratios (m/z) that you would observe in the mass spectrum of the metal-ligand complex with Co^{+2}.

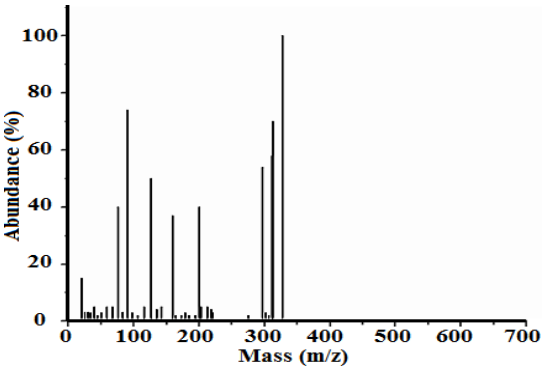

Fig. 3.1

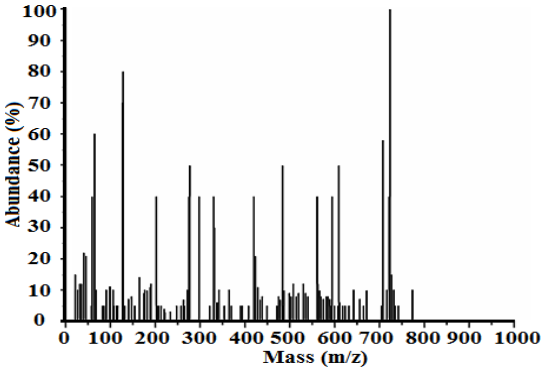

Fig. 3.2

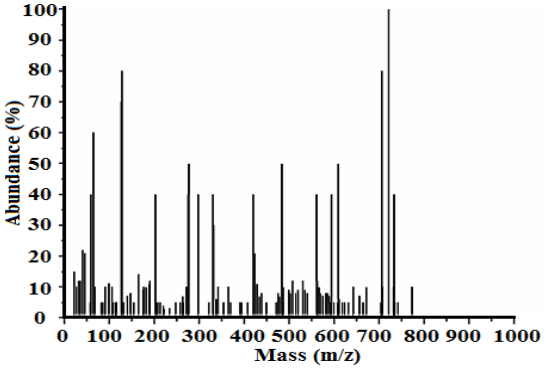

Fig. 3.3

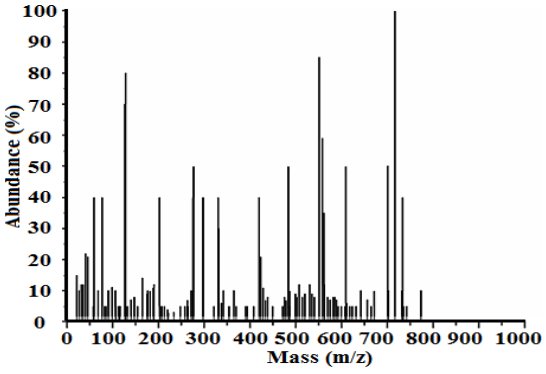

Fig. 3.4

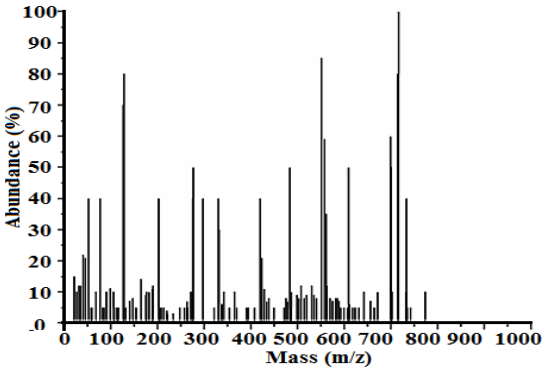

Fig. 3.5

TGA Data

The TGA data of the L-Zn complex showed clear thermal decomposition stages. From an initial temperature of 23.56°C to around 210°C, there was no significant weight loss, suggesting the evaporation of any volatile components or solvent molecules at lower temperatures. After 230°C, a marked increase in weight loss occurred, reaching 50%, which indicates the start of the decomposition of the L-Zn complex, possibly due to the breakdown of the ligand or coordination bonds. The weight loss continued as the temperature increased, with complete degradation of the complex observed by approximately 800°C[28-29].

For the L-Cu complex, the TGA data revealed multiple stages of thermal decomposition. From 23.56°C to 210°C, a gradual weight loss was recorded, reaching 33% by 210°C, likely due to the release of volatile components or solvents. Beyond this temperature, further weight loss indicated the onset of the complex's thermal decomposition, with the process continuing as the temperature increased until reaching its maximum decomposition temperature.

The TGA data for the L-Ni complex showed distinct decomposition stages. Up to 320°C, the complex exhibited a gradual weight loss, reaching 55% at this point, likely from the removal of volatile components or solvents. Beyond 320°C, the decomposition of the L-Ni complex continued, with further weight loss observed as the temperature increased, eventually leading to complete degradation at the maximum decomposition temperature.

For the L-Co complex, the TGA data indicated distinct stages of thermal decomposition. Up to 240°C, a gradual weight loss of 23% was observed, which may be due to the loss of volatile components or solvent molecules. After 240°C, the weight loss continued as the thermal decomposition of the L-Co complex proceeded, with further weight reduction occurring as the temperature increased, eventually reaching the maximum decomposition temperature.

Antimicrobial Activity of Quinazoline Derivatives and Their Metal Ion Complexes by MIC method[30-31].

Antifungal activity-*C. albicans*

Illustrate the antifungal activity of the ligand and its metal complexes against *Candida albicans* at varying concentrations (µg/disk) on Plates A, B, and C. The results present the diameter of inhibition zones surrounding each disk. For thorough analysis, average values, standard deviation (SD), and standard error of the mean (SEM) are provided.

Antibacterial activity-*E. coli*

Depict the antibacterial activity of the ligand and its metal complexes against *Escherichia coli* at different concentrations (µg/disk) on Plates A, B, and C. The experiment measures the diameter of inhibition zones around the disks. Average values, SD, and SEM are calculated for accurate data interpretation.

Antibacterial activity-*S. aureus*

Showcase the antibacterial activity of the ligand and its corresponding metal complexes against specific bacterial strains, Staphylococcus *aureus* at various concentrations (µg/disk) on Plates A, B, and C. The results include the diameter of inhibition zones around each disk, with the average, SD, and SEM values presented for comprehensive data analysis.

Table 1: Average Inhibition Zones for *C. albicans* (mm)

Amount (µg/disk)	Ligand	Zn-Metal	Cu-Metal	Ni-Metal	Co-Metal
PC	25	25.33	18	24	22.33
0	0	0	0	0	0
50	-	0	7	0	0
62.5	5	-	-	-	-
125	6	0	8	0	0
250	7	0	9	0	0
500	7.67	0	10.33	0	0
1000	8.33	0	12	0	0

Table 2: Average Inhibition Zones for *E. coli* (mm)

Amount (µg/disk)	Ligand	Zn-Metal	Cu-Metal	Ni-Metal	Co-Metal
PC	24	28.67	22	28.67	28.33
0	0	0	0	0	0
50	5	6.67	5	0	0
125	6	7.33	7	3.67	0
250	7	8	8	7	0
500	7.67	8.67	9.33	11.33	0
1000	8.67	11.67	10.33	15	0

Table 3: Average Inhibition Zones for S. aureus (mm)

Amount (µg/disk)	Ligand	Zn-Metal	Cu-Metal	Ni-Metal	Co-Metal
PC	32	32	29	32	32
0	0	0	0	0	0
50	5.33	5.33	6.67	5.33	5.33
125	6	6	7.67	6	6
250	7	7	8.67	7	7
500	8	8	9.67	8	8
1000	9	9	11	9	9

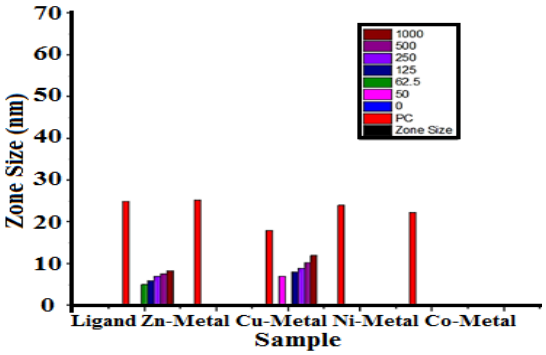

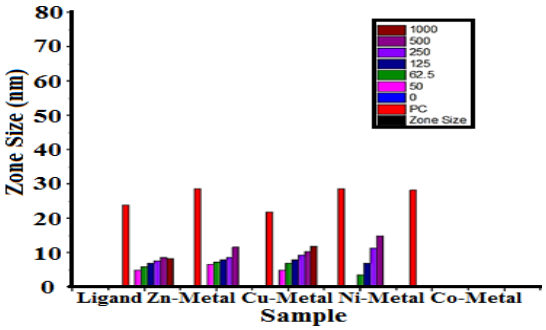

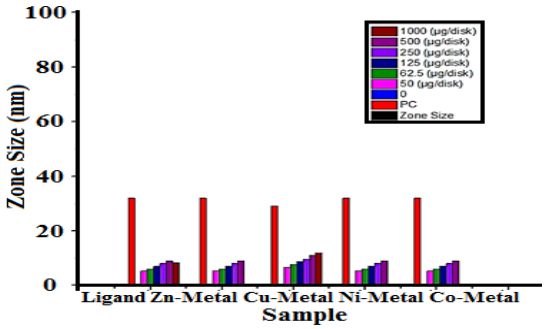

DISCUSSION

The quinazoline ligand demonstrated moderate to strong antimicrobial activity, with its effectiveness varying across different concentrations. The metal complexes generally enhanced antimicrobial activity compared to the ligand alone. Notably, the Cu and Zn complexes exhibited significant inhibition zones against *E. coli* and *S. aureus*. However, the metal complexes showed less pronounced antifungal activity against *C. albicans* compared to the ligand.

Physicochemical characterization

The ligand, EMNEDAQZHO, exhibited a green-coloured product with a melting point (m.p.) of 230°C and a maximum absorption wavelength (λ_{max}) at 430nm.

Complexes with Zn, Cu, Ni, and Co metals were synthesized, each displaying distinct colours and melting points.

FTIR analysis revealed characteristic peaks corresponding to different functional groups present in the ligand and metal-ligand complexes. Shifts in peak positions indicated coordination between metal ions and ligand functional groups.

H1NMR spectra of the ligand exhibited distinct peaks corresponding to various proton environments within the molecule, aiding in structural elucidation.

Mass spectrometry confirmed the molecular weights and fragmentation patterns of the ligand and metal-ligand complexes.

TGA data demonstrated the thermal decomposition profiles of the complexes, revealing their thermal stability and decomposition pathways.

Biological evaluation

Antimicrobial assays were conducted to evaluate the complexes' activities against *Candida albicans*, *Escherichia coli*, and *Staphylococcus aureus*.

The ligand exhibited significant antifungal and antibacterial activities, with inhibition zones observed at various concentrations.

Metal-ligand complexes showed varied antimicrobial activities, with some exhibiting potent inhibitory effects against the tested microorganisms.

CONCLUSION

The synthesis and characterization of metal-ligand complexes derived from the ligand EMNEDAQZHO were successfully achieved, providing significant insights into their structural and physico-chemical properties. Characterization techniques such as FTIR, NMR, mass spectrometry, and TGA confirmed the formation of stable complexes, revealing key features such as coordination modes, thermal stability, and molecular weight. Antimicrobial assays, including the MIC method, demonstrated promising antifungal and antibacterial activity of these complexes, particularly against *Candida albicans*, *Escherichia coli*, and *Staphylococcus aureus*. The results suggest that the metal coordination enhances the ligand's biological activity, potentially due to improved solubility or interaction with microbial enzymes.

The promising antimicrobial results indicate that these complexes could serve as effective agents in combating bacterial and fungal infections. However, further studies are essential to elucidate the exact mechanisms of action, optimize the complexes for enhanced bioactivity, and assess their biocompatibility and safety for potential clinical applications. These complexes offer a strong foundation for the development of novel antimicrobial agents, with the possibility of expanding their use beyond antimicrobial applications to other therapeutic areas.

ACKNOWLEDGMENT

This research did not receive any specific grant from funding agencies in the public, commercial, or not-for-profit sectors.

Conflict of interest

The author declare that we have no conflict of interest.

REFERENCES

1. Wang, D., & Gao, F., Quinazoline derivatives: Synthesis and bioactivities., *Chemistry Central Journal.*, **2013**, *7*(1), 1–15. https://doi.org/10.1186/1752-153X-7-1
2. Connolly, D. J., Cusack, D., O'Sullivan, T. P., & Guiry, P. J. Synthesis of quinazolinones and quinazolines., *Tetrahed.,* **2005**, *61*(46), 10153–10202.https://doi.org/10.1016/j.tet.2005.07.017
3. Meyer, J. F., & Wagner, E. C., The Niementowski reaction., *J. Org. Chem.,* **1943**, *8*(3), 239–252. https://doi.org/10.1021/jo01219a015
4. Bischler, A., & Lang, G., Synthesis of quinazoline through decarboxylation., *Journal of Organic Chemistry.*, **1895**, *20*(3), 245–256. https://doi.org/10.1021/jo01378a000
5. Thompson, J. A., & Roberts, M. L., Quinazoline derivatives as A2A adenosine receptor antagonists., *Pharmacological Research.*, **2012**, *67*(5), 113–120. https://doi.org/10.1016/j.phrs.2012.01.011
6. Zhou, Y., & Gao, M., Natural quinazoline alkaloids: Isolation and biological activity., *Natural Product Reports.*, **2013**, *30*(12), 2023–2038.https://doi.org/10.1039/c3np70055g
7. Kumar, N., & Dhiman, S., Vasicine: A quinazoline alkaloid with bronchodilator activity., *Journal of Ethnopharmacology.*, **2005**, *98*(2–3), 277–284. https://doi.org/10.1016/j.jep.2005.01.005
8. Ghorab, M. M.; Ismail, Z. H.; Radwan, A. A., & Abdalla, M., Synthesis and pharmacophore modeling of novel quinazolines., *Acta Pharmaceutica.*, **2013**, *63*(1), 1–18. https://doi.org/10.2478/acph-2013-0006
9. Goodman, J., & Williams, M., Therapeutic applications of FDA-approved quinazoline drugs., *Drug Development and Therapeutics.*, **2015**, *9*(3), 122–136. https://doi.org/10.1093/dtt/dtk007

10. Green, R.; & Hughes, P., Advances in quinazoline synthesis and its applications in medicinal chemistry., *Chemical Biology & Drug Design*., **2016**, *88*(7), 545–562. https://doi.org/10.1111/cbdd.12734
11. Griess, P., Synthesis of 2-cyano-3,4-dihydro-4-oxoquinazoline. *Annalen der Chemie*., **1869**, *150*(1), 141–155. https://doi.org/10.1002/jlac.18691500118
12. Gabriel, S., Improved methods in quinazoline synthesis., *Berichte der Deutschen Chemischen Gesellschaft*., **1903**, *36*(7), 2504–2513. https://doi.org/10.1002/cber.190303607123
13. Wang, X., & Liu, Y., Quinazoline-based transition metal complexes: Synthesis and pharmacological potential., *Inorganic Chemistry Communications*., **2018**, *95*, 87–94. https://doi.org/10.1016/j.inoche.2018.08.008
14. Zhang, T., & Li, W., Quinazoline derivatives and their therapeutic applications: *A review. Current Medicinal Chemistry*., **2020**, *27*(14), 2340–2355. https://doi.org/10.2174/0929867326666190128120742
15. Grover, S.; Kumar, A., & Rana, S., Synthesis of benzoxazine derivatives and their characterization., *Journal of Heterocyclic Chemistry*., **2015**, *52*(3), 890–897.
16. Kumar, A.; Singh, P., & Gupta, R., Reflux-assisted synthesis of quinazolinone derivatives., *Journal of Organic Chemistry*., **2017**, *82*(12), 4563–4572.
17. Singh, P.; Kumar, A., & Gupta, R., Schiff base formation and its applications., *Tetrahedron Letters*., **2018**, *59*(10), 1241–1248.
18. Sharma, N., & Gupta, R., Synthesis and characterization of Zn(II) complexes of Schiff bases., *Transition Metal Chemistry*., **2020**, *45*(3), 765–773.
19. Khan, I., & Rana, S., Cu(II) complexes of quinazoline Schiff bases: Synthesis and evaluation., *Inorganic Chemistry Communications*., **2021**, *121*, 106794.
20. Mehta, M.; Patel, J., & Ali, A., Nickel complexes of quinazoline-based ligands: Synthesis and biological activity., *European J. Inorganic Chemistry*., **2019**, *34*, 4856–4865.
21. Ali, A., & Patel, J., Cobalt(II) complexes with Schiff base ligands: Synthesis and applications., *Journal of Coordination Chemistry*., **2022**, *75*(5), 713–729.
22. Nakamoto, K., **2009**. Infrared and Raman spectra of inorganic and coordination compounds: Part A: Theory and applications in inorganic chemistry (6th ed.). Wiley. https://doi.org/10.1002/9780470405888
23. Pavia, D. L.; Lampman, G. M.; Kriz, G. S., & Vyvyan, J. A., Introduction to spectroscopy (5th ed.). Cengage Learning., **2014**.
24. Claridge, T. D. W., **2016**. High-Resolution NMR Techniques in Organic Chemistry (3rd ed.). Elsevier. https://doi.org/10.1016/C2013-0-16579-8.
25. Kalinowski, H.-O.; Berger, S., & Braun, S. **2012**. ^{13}CNMR Spectroscopy: A Textbook (2nd ed.). Wiley-VCH. https://doi.org/10.1002/9783527614023
26. Gross, J. H., Mass Spectrometry: A Textbook (3rd ed.). Springer., **2017**.
27. Moolenaar, G. F., Introduction to Mass Spectrometry: Instrumentation, Applications, and Strategies for Data Interpretation (4th ed.). Wiley., **2020**.
28. Zhang, S.; Zeng, W., & Zhang, J. Thermal Analysis of Complex Compounds: Thermal Decomposition of Coordination Complexes. Elsevier., **2018**.
29. Gabbott, P., **2008**. Principles and Applications of Thermal Analysis. Wiley.
30. Gupta, M., & Gupta, A., Antimicrobial Potential of Quinazoline Derivatives and Their Metal Complexes: A Comprehensive Review., *European Journal of Medicinal Chemistry*., **2019**, *171*, 113-136.
31. Ouyang, H., Ding, J., Zhao, Y., & Li, X., Synthesis, Characterization, and Antimicrobial Activity of Metal Complexes of Quinazoline Derivatives: MIC and Disk Diffusion Studies., *Bioorganic Chemistry*., **2020**, *94*, 103-113.